Micro and Nanostructures 212 (2026) 208567

Contents lists available at ScienceDirect

Micro and Nanostructures

journal homepage: www.journals.elsevier.com/micro-and-nanostructures

Weakening of the internal strain field in InAs/GaAs submonolayer quantum dots due to indium segregation

T.F. Cantalice, S.M. Urahata, A.A. Quivy *

Institute of Physics, University of São Paulo, rua do Matão, 1371, Cidade Universitária, 05508-090, São Paulo, Brazil

ARTICLE INFO

Keywords:
InAs/GaAs
Segregation
Simulations
Strain
Quantum dots
Submonolayer

ABSTRACT

InAs/GaAs submonolayer quantum dots rely on the vertical alignment of two-dimensional InAs islands separated by thin GaAs layers. These stacks arise from the local strain field generated by the lattice mismatch between the constituent materials. However, experimental observations show that such quantum dots appear irregular and shorter than expected. Indium segregation is particularly strong in the InAs/GaAs system and is suspected to weaken the internal strain field. To confirm this assumption, we simulated the strain in the GaAs matrix surrounding InAs inclusions with the shape of either a full sphere or a thin truncated hemisphere. The results demonstrate that, when the original two-dimensional InAs islands are realistically represented by a thin truncated hemisphere subjected to strong In segregation, the internal strain is indeed much lower than that required to form full stacks, even for distances as short as a few monolayers between inclusions.

1. Introduction

In recent years, submonolayer quantum dots (SMLQDs) have gained increasing attention, as they are expected to overcome most of the drawbacks of conventional Stranski–Krastanov quantum dots (SKQDs), e.g., the lack of control of their height, their relatively low areal density, and the presence of a wetting layer that introduces extra strain and contributes to weakening carrier confinement. Unlike SKQDs, which result from the growth of a few monolayers of strained material that relax and form three-dimensional (3D) islands at the surface, SMLQDs are obtained by alternating the deposition of a fraction of a single atomic layer of strained material and a few atomic layers of another material [1]. For the InAs/GaAs system, SKQDs are formed when more than 1.7 monolayers (MLs) of InAs are deposited on a GaAs(001) surface [2] — one can go up to 3 MLs without generating an excessive number of defective islands — whereas SMLQDs are commonly obtained by depositing 0.3-0.5 ML of InAs followed by 1-5 MLs of GaAs [3]. When a submonolayer of InAs is deposited on the GaAs(001) surface in the right conditions [4,5], tiny two-dimensional (2D) InAs islands are nucleated and can reach a density [1,3] as high as 10^{12} cm^{-2}. After being covered, these islands generate a tensile strain laterally at the surface of the GaAs layer, resulting from the larger lattice parameter of InAs when compared to GaAs. As a consequence, when the next fraction of InAs monolayer is deposited, its 2D InAs islands will preferentially nucleate on top of those of the previous InAs submonolayer, where the in-plane GaAs lattice parameter is slightly larger. By repeating this growth sequence several times, one can possibly obtain stacks of 2D InAs islands that behave as individual quantum dots. Ultimately, the density of SMLQDs is expected to be similar to that of 2D InAs islands nucleated on the GaAs surface, their height can be tuned by carefully choosing the number of repetitions [6,7], and no wetting layer will ever form, as the amount of InAs material deposited in each cycle is always lower than a monolayer.

* Corresponding author.
E-mail address: aquivy@if.usp.br (A.A. Quivy).

https://doi.org/10.1016/j.micrna.2026.208567
Received 6 November 2025; Received in revised form 19 December 2025; Accepted 6 January 2026
Available online 7 January 2026

SMLQDs grown in this way have already been shown to provide carrier confinement, allowing for the improvement of devices previously based on SKQDs [8–15]. However, recent results suggest that current InAs/GaAs SMLQDs are far from the ideal picture, where they are always sketched as regular stacks of 2D InAs islands separated by thin GaAs layers [16–18]. The expected vertical alignment of the 2D islands in consecutive InAs submonolayers results from the well-known experimental fact that InAs SKQDs do stack vertically when they are grown in successive InAs layers separated by less than 10 nm of GaAs material [19,20]. Since the 2D InAs islands of a SMLQD are separated by a few monolayers of GaAs only, one could indeed infer that such vertical stacking should also occur in SMLQDs. However, high-resolution cross-sectional scanning tunneling microscopy (XSTM) images revealed that, instead of vertical stacks of 2D InAs islands, these InAs/GaAs SMLQDs actually look like irregular In-rich $In_xGa_{1-x}As$ clusters scattered in a thick $In_yGa_{1-y}As$ layer containing a lesser amount of In (x>y) [16]. Additionally, these clusters exhibit no evidence of 2D InAs islands — or of any remaining internal periodicity — and they are always shorter than expected from the number of repetitions. This is most probably due to In segregation [16–18] which is known to be very strong in the InAs/GaAs system and can remove approximately 80% of the In atoms from their original incorporation site and spread them into the next layers to be grown [17,21–23]. Since the original 2D InAs islands lose many In atoms and are replaced by 2D $In_xGa_{1-x}As$ islands, one could wonder whether the strain field around them is still strong enough to effectively influence the nucleation of the 2D islands of the next InAs submonolayer. Moreover, considering that segregation transfers most In atoms to the GaAs matrix around the 2D islands, the local strain is further reduced.

In this paper, we used a formalism developed by Kolesnikova et al. [24] to estimate the strain in the GaAs matrix surrounding InAs inclusions, in the presence and absence of In segregation. Inclusions having the shape of a sphere were initially considered to validate our results and compare them to those of Xie et al. [19] Then, more emphasis was given to truncated hemispheres — looking like thin circular slices — to describe the 2D InAs islands more realistically.

2. Numerical method

In their pioneering study of the vertical alignment of SKQDs in consecutive InAs layers separated by GaAs material, Xie et al. [19] simulated the elastic properties of SKQDs and approximated their lens-shaped geometry by a small sphere having the same volume of InAs material. With this simple geometry, the radial strain ϵ_{RR} generated by the InAs inclusions in the surrounding GaAs matrix could be calculated analytically as [19,25]

$$\epsilon_{RR} = \frac{3B_{InAs}\epsilon_0}{3B_{InAs} + 2E_{GaAs}/(1+\nu_{GaAs})}\left[-2\left(\frac{R_0}{R}\right)^3\right] \quad (1)$$

where B, ϵ_0, E, and ν are, respectively, the Bulk modulus, lattice mismatch, Young's modulus, and Poisson's ratio of the referred materials, while R_0 and R are the radius of the equivalent sphere and distance between the center of the sphere and the position in the GaAs matrix where the strain is evaluated ($R > R_0$). Then, they calculated the probability of getting vertically aligned SKQDs in consecutive InAs layers, and deduced an analytical expression providing the maximum distance z_0 between two consecutive InAs layers for which this probability was at least 95%. For typical InAs SKQDs, represented by spheres with radius $R_0 = 3.7$ nm, they obtained $z_0 = 35.6$ MLs (≈ 10 nm). This implies that, for separations shorter than 10 nm, nearly all SKQDs in consecutive InAs layers should vertically align, whereas for distances larger than 200 MLs (≈ 57 nm), their calculations indicated that the nanostructures in adjacent InAs layers should be uncorrelated.

Although it may be acceptable to simulate three-dimensional lens-shaped SKQDs using spheres with the same volume, this approximation becomes more questionable when SMLQDs are considered. Indeed, XSTM images have shown that the In-rich clusters detected in SMLQDs samples have an approximate lateral size of 5 nm, which suggests that the original 2D InAs islands might be thin structures having an approximate diameter and height of 5 nm and 0.28 nm, respectively [3,16]. According to the model of Xie et al. [19], the volume of such a 2D island would then be equivalent to that of a sphere with a radius $R_0 = 1.1$ nm, which does not provide an accurate representation of the original 2D island. A disk or thin cylinder would be a more appropriate approximation. However, in order to keep the same spherical symmetry as Xie et al. [19] and allow further comparison with their model and data, we chose a slice of a sphere (truncated hemisphere). Obviously, for the very thin 2D islands investigated here (5 nm wide and only 0.28 nm high), this is very close to a disk.

To perform the simulations, we used the formalism developed by Kolesnikova et al. [24] who calculated the elastic field of dilatational inclusions (DIs) built from circular dilatational disks distributed continuously along an axis of symmetry. The advantage of such a model is that it is possible to calculate strain inside and outside inclusions having different shapes through analytical solutions obtained by computing Lipschitz–Hankel integrals or Lur'e series. The geometry used here to calculate the strain in the GaAs matrix around a 2D InAs island is illustrated in Fig. 1. It shows the generic problem of a DI with the shape of a slice of a sphere (truncated sphere) having a radius R_0, where $z_1 = R_0\cos\theta_1$ and $z_2 = R_0\cos\theta_2$ are the z values of the bottom and top parts of the truncated sphere. Given that the problem is symmetric around axis z, it can be solved in a plane (the sphere of Fig. 1 is projected in the xz plane) — with no need of the azimuthal angle ϕ of usual spherical coordinates — and readily extended to three dimensions due to the axial symmetry. The specific geometry adopted in the present work is actually a thin truncated hemisphere, where $\theta_1 = \pi/2$, $z_1 = 0$, $\theta_2 = \pi/2 - \arcsin(z_2/R_0)$, and $z_2 = h_{GaAs}$, with h_{GaAs} being the lattice parameter of GaAs (0.28 nm). In the case of 2D InAs/GaAs islands, the inclusion (gray truncated sphere) is made of InAs, while regions I and II are made of GaAs. The objective of the calculations is thus to estimate the strain in regions I (i.e., inside the sphere of radius R_0 but outside the inclusion) and II (outside the sphere) to check if it is strong enough to align the 2D islands from the next fraction of InAs layer that will be deposited just a few monolayers above.

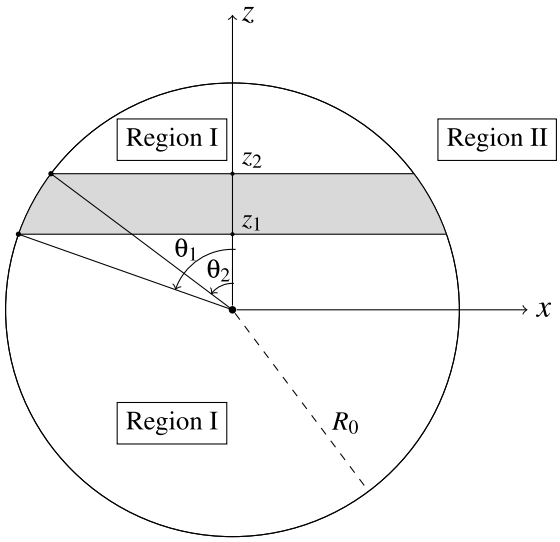

Fig. 1. Projection in the xz plane of a sphere of radius R_0 and a generic inclusion inserted in it — consisting of a thin horizontal slice of the sphere — together with their relevant parameters. The inclusion (gray) is made of InAs, while region I (inside the sphere) and region II (outside the sphere) are made of GaAs.

With this configuration, the strain in regions I and II can be estimated as [24]

$$\epsilon_{RR} = \frac{(1+\nu)\epsilon_0}{2(1-\nu)} \begin{cases} \sum_{n=2}^{\infty} B_n n(n-1)\left(\frac{R}{R_0}\right)^{n-2} P_n(\cos\theta), & \text{Region I} \\ \sum_{n=0}^{\infty} D_n (n+1)(n+2)\left(\frac{R_0}{R}\right)^{n+3} P_n(\cos\theta) & \text{Region II} \end{cases} \tag{2}$$

$$B_n = \frac{1}{(2n-1)}\left[\frac{1}{(2n+1)}P_{n+1}(t_0) - \frac{2(2n-1)}{(2n+1)(2n-3)}P_{n-1}(t_0) + \frac{1}{(2n-3)}P_{n-3}(t_0)\right]\Bigg|_{\cos\theta_1}^{\cos\theta_2} \tag{3}$$

$$D_n = \frac{1}{(2n+3)}\left[\frac{1}{(2n+5)}P_{n+3}(t_0) - \frac{2(2n+3)}{(2n+5)(2n+1)}P_{n+1}(t_0) + \frac{1}{(2n+1)}P_{n-1}(t_0)\right]\Bigg|_{\cos\theta_1}^{\cos\theta_2} \tag{4}$$

In Eqs. (2)–(4) above, $P_n(t_0)$ are Legendre polynomials, and $t_0 = \cos\theta_1$ or $\cos\theta_2$, where $\cos\theta_1$ and $\cos\theta_2$ are the inferior and superior limits of B_n and D_n. It means that B_n must be calculated as $B_n(\cos\theta_2) - B_n(\cos\theta_1)$, and the same applies to D_n.

Although 2D InAs islands formed during submonolayer growth on GaAs(001) are known to exhibit anisotropic shapes and elongation due to surface reconstruction and diffusion anisotropy [4], their defining morphological feature is their extremely small aspect ratio, with a lateral size of a few nanometers and a thickness of one monolayer. In this limit, a disk-like geometry provides an appropriate continuum representation of the islands. We therefore model these 2D islands as thin truncated hemispheres, which are geometrically equivalent to disks for the dimensions considered here, while preserving axial symmetry. This choice enables a direct comparison with earlier spherical models [19] and allows the use of the analytical formalism of Kolesnikova et al. [24], without affecting the qualitative or quantitative conclusions regarding the strain field.

3. Results and discussion

Before starting the simulations of interest, we verified whether the formalism introduced by Kolesnikova et al. [24] was equivalent to that used by Xie et al. [19] when the inclusion is a full sphere. In that case, all the solutions of the problem belong to region II, $\theta_1 = \pi$, $\theta_2 = 0$, $D_0 = -2/3$, and $D_n = 0$ for $n > 0$. Substituting these values in Eqs. (2) and (4), one obtains

$$\epsilon_{RR} = \frac{(1+\nu)\epsilon_0}{3(1-\nu)}\left[-2\left(\frac{R_0}{R}\right)^3\right] \tag{5}$$

The elastic properties of isotropic and homogeneous materials in the linear deformation regime can be described in several ways, depending on the elastic constants employed. For instance, the coefficient of Eq. (5) can be rewritten as [26]

$$\frac{(1+\nu)}{3(1-\nu)} = \frac{B}{M} = \frac{B}{B+4G/3} = \frac{3B}{3B+2E/(1+\nu)} \tag{6}$$

where M and G are respectively the longitudinal and shear moduli. Replacing the coefficient of Eq. (5) with the right member of Eq. (6) leads to an expression that is identical to Eq. (1), confirming that, for a sphere, both formalisms are similar, and that the model of Kolesnikova et al. [24] was successfully implemented.

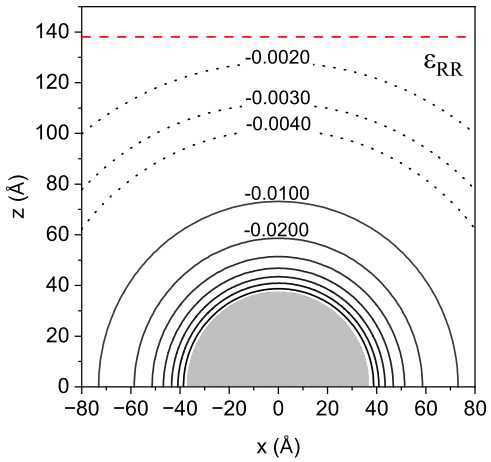

Fig. 2. Distribution of the radial strain ϵ_{RR} in the GaAs matrix surrounding a spherical InAs inclusion (gray) of radius $R_0 = 3.7$ nm, as done in the work of Xie et al. to simulate an InAs SKQD [19]. The horizontal red dashed line represents the GaAs surface, located 10 nm above the top of the InAs sphere, where a SKQD of the next InAs layer is expected to nucleate. These authors showed that this is the thickest GaAs spacer for which the probability to vertically align SKQDs in consecutive InAs layers is at least 95%. The increment between adjacent solid isostrain lines is 0.01.

The next step would consist in using Eqs. (2)–(4) to compute the strain in the GaAs material surrounding the 2D InAs islands, with and without segregation. However, since the objective is to compare the strain field around a large 3D InAs SKQD and a small 2D InAs island, it is first necessary to evaluate the strain in the GaAs matrix, 10 nm above an InAs SKQD, as this is the distance below which such nanostructures are almost always vertically aligned in consecutive InAs layers. This value will then be compared to the strain computed a few monolayers above a 2D InAs island to determine if the latter is large enough to promote their effective stacking. Therefore, initially, we used the model of Kolesnikova et al. [24] to calculate the radial strain in the GaAs matrix surrounding a spherical InAs inclusion, as done by Xie et al. [19]. The results of the calculations are shown in Fig. 2. As the inclusion is spherical and the elastic properties of both InAs and GaAs are isotropic, one expects the strain distribution to show spherical symmetry. One can see in the top part of the figure that $\epsilon_{RR} = -0.00159$ in the GaAs matrix at a distance $z_0 = 35.6$ MLs (≈ 10 nm) above the surface of the sphere. This value is negative because the GaAs material surrounding the InAs inclusion is stretched (positive tensile strain) in the plane perpendicular to the radial direction, owing to the larger lattice parameter of InAs. As a consequence, because of the tetragonal deformation of the GaAs unit cell, the GaAs matrix is compressively strained along the radial direction, leading to negative values of ϵ_{RR}. This numerical value will be used later as a reference to assess whether vertical alignment of the different types of nanostructures investigated here can be expected. The most relevant strain data for this study are reported in Table 1.

As already mentioned previously, representing a 5 nm-wide 2D InAs island by a small sphere of radius of 1.1 nm might not be realistic. Fig. 3 shows that the strain in the GaAs matrix at a distance of 2 MLs above the surface of an InAs spherical inclusion is −0.0245, i.e., more than fifteen times larger than that needed to fully align SKQDs separated by 10 nm. It is consistent with the value of $z_0 = 14.6$ MLs for that specific configuration, as calculated with the formalism of Xie et al. [19]. As z_0 is much larger than the distance of 2 MLs separating two consecutive InAs submonolayers, it means that the strain calculated in Fig. 3 should be more than sufficient to fully align 2D InAs islands and form tall SMLQDs. However, this is not observed experimentally, as revealed by XSTM images [16]. One could therefore infer that the spherical model is indeed a poor representation, although neglecting In segregation may also partly account for this discrepancy. The strain value mentioned above was calculated at a distance of 2 MLs instead of 2.5 MLs because, even if the SMLQDs investigated here are formed by the cyclic deposition of 0.5 ML of InAs followed by 2.5 MLs of GaAs, half a layer of GaAs is used to fill in the space between the 2D InAs islands (completing the first monolayer). Therefore, only 2 MLs of GaAs will actually cover and separate them from the 2D islands of the next InAs submonolayer.

When the same geometry is analyzed in the presence of In segregation, the situation improves. Indium segregation during InAs deposition on a GaAs(001) surface has been widely reported, with segregation coefficients typically ranging between 0.7 and 0.9 [16,17,21–23,27,28]. At the growth temperature used here as a reference (500 °C), several independent measurements consistently yield $R_{seg} \approx 0.8$. It means that, when the 2D InAs islands are covered by GaAs, only 20% of the In atoms remain in the original 2D islands, while the rest of them move with the growth front (adsorbed on the surface as mobile species) and are slowly incorporated into the subsequent GaAs layers. For the SMLQD structure investigated here — consisting of 6 repetitions of 0.5 ML of InAs followed by 2.5 MLs of GaAs — the phenomenological segregation model of Muraki [21] shows that the In content in the next two GaAs layers just above the 2D islands will be 16% and 13% (supposing segregation happens only vertically). The other In atoms that have not been incorporated into the 2D islands, nor into the thin GaAs layers, will accumulate at the surface (51% of the original In atoms) and add to the fraction of the In monolayer in the next cycle, leading to a second layer of 2D islands containing

Table 1
Radial strain value ϵ_{RR} above the center of the inclusion as a function of the model that was used and distance from the inclusion's surface. z_0 can only be calculated when the inclusion is a full sphere, as proposed by Xie et al. [19]. R_0 and h are the sphere radius and the height (thickness) of the truncated hemisphere used to simulate a 2D island. When segregation is neglected, the segregation coefficient R_{seg} is zero. A negative value of ϵ_{RR} means that the material is under compressive strain along the radial direction.

Model	ϵ_{RR}	Distance (MLs)	z_0 (MLs)
Fig. 2[a]	−0.00159	35.6	35.6
Fig. 3[b]	−0.02450	2	14.6
Fig. 5[c]	−0.00220	2	2.8
Fig. 6[d]	−0.00590	2	
Fig. 7[e]	−0.00054	2	

[a] 3D InAs SKQD, sphere $R_0 = 3.7$ nm, $R_{seg} = 0$.
[b] 2D InAs island, sphere $R_0 = 1.1$ nm, $R_{seg} = 0$.
[c] 2D InGaAs island, sphere, $R_0 = 1.1$ nm, $R_{seg} = 0.8$.
[d] 2D InAs island, truncated hemisphere $R_0 = 2.5$ nm, $h = 0.28$ nm, $R_{seg} = 0$.
[e] 2D InGaAs island, truncated hemisphere $R_0 = 2.5$ nm, $h = 0.28$ nm, $R_{seg} = 0.8$.

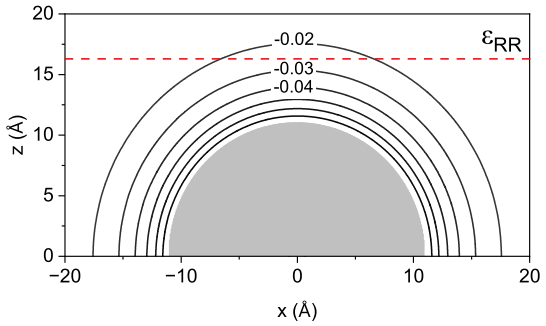

Fig. 3. Distribution of the radial strain ϵ_{RR} in the GaAs matrix surrounding a spherical InAs inclusion (gray) of radius $R_0 = 1.1$ nm to simulate a 2D InAs island having a lateral size and height of 5.0 nm and 0.28 nm, respectively. The horizontal red dashed line represents the GaAs surface, located 2 MLs (0.56 nm) above the top of the InAs sphere, where a 2D island of the next InAs submonolayer is supposed to nucleate to form a SMLQD. The increment between adjacent solid isostrain lines is 0.01.

30% of In. Fig. 4 shows that the In content keeps increasing slowly, while growth proceeds, reaching 40% in the 2D islands and 32% in the thin GaAs monolayers of the sixth cycle (blue curve). Therefore, the situation is very different from the nominal case, where the 2D islands are assumed to be made of InAs and are separated by GaAs material (black dashed curve). When segregation is taken into account, the average In content of such SMLQDs is close to 28% (instead of 33% when segregation is neglected), and the local In composition varies between 13% and 40% only, instead of 0% and 100% in the nominal case. The In atoms that are still adsorbed on the surface at the end of the sixth repetition will be progressively incorporated into the GaAs cap layer, giving rise to the tail observed in Fig. 4 for x values larger than 18.

We have already reported elsewhere [16] that XSTM data of SMLQDs consisting of 6 repetitions of 0.5 ML of InAs followed by 2.5 MLs of GaAs, similar to those investigated here, revealed In-rich clusters scattered in a thick layer having a composition of approximately $In_{0.2}Ga_{0.8}As$ and $In_{0.1}Ga_{0.9}As$, respectively. It means that part of the In atoms that segregate from the original 2D InAs islands also diffuse laterally on the surface and incorporate out of the SMLQDs to form the thick $In_{0.1}Ga_{0.9}As$ layer around them. To take this into account in our calculations, 20% of the In atoms were allowed to diffuse horizontally during the segregation process in each layer of the deposition cycle. By doing so, the overall In concentration in the SMLQDs was reduced from 28% to 20%, and the In concentration in the matrix around them increased from 0% to 11%, in excellent agreement with the XSTM data. This value of 20% was therefore not arbitrarily chosen, but is instead experimentally constrained to reconcile Muraki's empirical model [21] — which accounts only for segregation along the growth direction — with high-resolution XSTM observations indicating that a significant fraction of In atoms diffuse laterally to form the $In_{0.1}Ga_{0.9}As$ matrix surrounding the SMLQDs [16]. According to Fig. 4 (red curve), in these conditions the In content of the 2D islands increases monotonically from 20% to 27% during the six repetitions (providing an average of 25% when all of them are taken into account), while the In content in the thin interlayers varied from 10% to 22%, with an average of 18%. Therefore, for the sake of simplicity, to simulate the strain above a 2D InAs island represented by

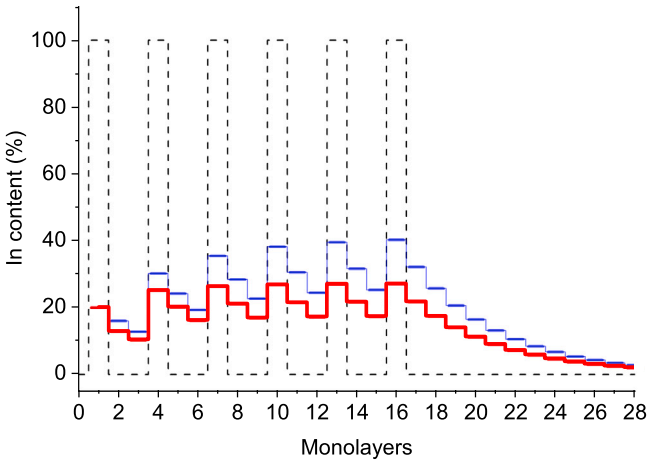

Fig. 4. In distribution inside a SMLQD consisting of 6 repetitions of 0.5 ML of InAs followed by 2.5 MLs of GaAs. The black dashed line represents the nominal situation where segregation is neglected ($R_{seg} = 0$). The thin blue curve shows the case where all In atoms segregate vertically (supposing $R_{seg} = 0.8$), i.e., remain inside the SMLQD. The thick red curve illustrates a more realistic situation, where some of the In atoms (20%) diffuse horizontally, i.e., leave the SMLQD to form the thick InGaAs layer around it. Layers 1–18 are inside the SMLQD, while layers 19–28 are part of the GaAs cap layer in which the In atoms, that are still adsorbed on the surface after the sixth repetition, will be progressively incorporated.

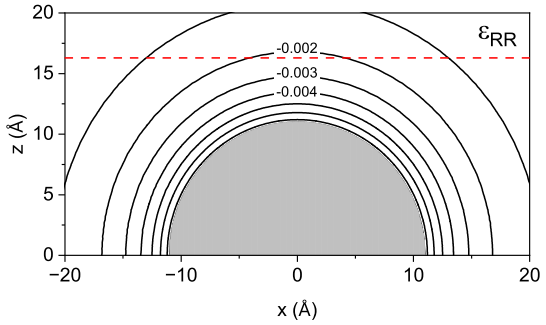

Fig. 5. Distribution of the radial strain ϵ_{RR} in the matrix surrounding a spherical inclusion (gray) of radius $R_0 = 1.1$ nm to simulate a 2D InAs island having a lateral size and height of 5 nm and 0.28 nm, respectively. Since here segregation was taken into account ($R_{seg} = 0.8$), the average compositions of the inclusion and matrix were estimated to be $In_{0.25}Ga_{0.75}As$ and $In_{0.18}Ga_{0.82}As$, respectively. The horizontal red dashed line represents the surface of the matrix located 2 MLs (0.56*nm*) above the top of the sphere, where a 2D island of the next InAs submonolayer is supposed to nucleate to form a SMLQD.

a sphere in the presence of segregation, that sphere should have a diameter of 1.1 nm, be made of $In_{0.25}Ga_{0.75}As$, and be separated from the next one on top (as in the SMLQD structure) by $In_{0.18}Ga_{0.82}As$ material. As expected, the strain distribution of such a configuration, shown in Fig. 5, is similar to that observed in Figs. 2 and 3, but the absolute strain values above the sphere are now lower, due to the smaller difference in In concentration between the sphere and its surroundings. Table 1 shows that, at a distance of 2 MLs above the inclusion's surface, the radial strain is −0.00220 and is associated with a value of $z_0 = 2.8$ MLs. Both values are larger than −0.00159 and 2.0 MLs (considering their absolute values), respectively, suggesting that such inclusions should still be able to form stacks. Although these numbers point in the right direction and are now close to the limit where the strain field might no longer be strong enough to provide full vertical alignment, such simulations, performed in the presence of segregation, are still not able to explain the experimental XSTM data of SMLQDs, which is probably, as suggested previously, an indication of the poor representation of a 2D island by a sphere.

We now turn to more realistic calculations to simulate the 2D islands, using thin slices of a sphere and employing the full potential of the model proposed by Kolesnikova et al. [24] To this end, we considered a truncated hemisphere of radius $R_0 = 2.5$ nm and height $h = 0.28$ nm to represent a 2D island. We started with inclusions containing only InAs and surrounded by GaAs, i.e., neglecting In segregation. As the inclusion is inscribed in a sphere, it was necessary to compute the strain in both regions I and II of Fig. 1. The results are shown in Fig. 6 where one can see that, for such a geometry, the strain distribution is now very different from that observed in the previous figures. There is no apparent discontinuity in the strain field near the border of the sphere — i.e., at the interface between regions I and II — confirming that Eqs. (2)–(4) are consistent and were well implemented. Far from the inclusion, the isostrain lines are approximately circular, suggesting that the 2D islands can eventually be simulated satisfactorily by small

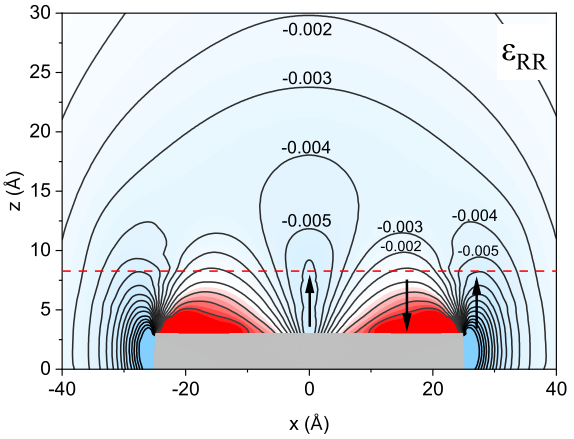

Fig. 6. Distribution of the radial strain ϵ_{RR} in the GaAs matrix surrounding a 2D InAs island represented by a thin truncated hemisphere (gray) of radius R_0 = 2.5 nm and height h = 0.28 nm. In segregation was neglected in the calculations (R_{seg} = 0). The red horizontal dashed line represents the surface of the GaAs matrix located 2 MLs (0.56 nm) above the top of the InAs inclusion, where a 2D island of the next InAs submonolayer is expected to nucleate to form a SMLQD. Red regions indicate tensile strain, i.e., $\epsilon_{RR} > 0$. The increment between adjacent solid isostrain lines is 0.001, and the arrows point toward more positive strain values.

spheres when strain is calculated far from them, as was done in the model of Xie et al. [19]. At very short distances, though — e.g., a few monolayers as in the case of vertical alignment of 2D islands to form SMLQDs — one can see that strain behaves in a very different way. When the 2D InAs islands are initially nucleated on the GaAs(001) surface, they experience biaxial strain from the GaAs substrate underneath, i.e., their material is compressed in the $x - y$ plane and is free to expand along the growth direction (z axis). Later, when they are covered, the GaAs material at their periphery is therefore under huge tensile strain along the z direction, resulting in a compressive strain along the radial direction, as shown by the high concentration of negative isostrain lines for $|x| > 25$Å. However, the relevant region for the present study is the one above the flat surface of the inclusion, as this is where a 2D island of the next InAs submonolayer is expected to nucleate to form a SMLQD. One can see that, close to the border of the 2D island, there is a GaAs region where the radial strain ϵ_{RR} is positive (red color in Fig. 6), meaning that the material is under compressive strain in the xy plane of the GaAs surface. Therefore, unlike the rest of the GaAs matrix, that region has a lateral lattice parameter that is smaller than that of unstrained GaAs, suggesting that it would be less energetically favorable to receive In adatoms [19]. But that region is close to the inclusion's surface, and what truly matters is the strain at the GaAs surface, 2 MLs above the inclusion (horizontal dashed line in Fig. 6), where the next InAs submonolayer will be deposited. At that distance, one can see that ϵ_{RR} reaches its most negative value (i.e., the lateral GaAs lattice parameter is under tensile strain and closer to that of InAs) exactly above the center of the island, which may thus act as an attraction center for In adatoms. There, $\epsilon_{RR} = -0.0061$, i.e., it is almost four times larger (in absolute value) than the strain needed to align 95% of conventional SKQDs. Consequently, according to these results, when the 2D islands are considered as truncated hemispheres and In segregation is neglected, one should also expect them to stack nicely and form regular SMLQDs, contradicting our experimental XSTM data. It is no longer possible to calculate z_0 in this case, as it was defined by Xie et al. [19] for a spherical inclusion only.

However, In segregation is very strong in the InAs/GaAs system, and any realistic calculation should also take it into account. As already done earlier for a sphere, we will now consider the 2D islands as thin truncated hemispheres made of $In_{0.25}Ga_{0.75}As$ surrounded by $In_{0.18}Ga_{0.82}As$ material. Fig. 7 shows that, when segregation is taken into account, the strain distribution does not change qualitatively, but the strain values are quantitatively different. As the InAs and GaAs materials of the nominal inclusion and matrix of Fig. 6 are replaced by $In_{0.25}Ga_{0.75}As$ and $In_{0.18}Ga_{0.82}As$, respectively, the local strain, which is related to the relative In content of both materials, should decrease. This can be seen in the strain distribution of Fig. 7, which has values about ten times smaller than in Fig. 6. More specifically, the region located 2 MLs above the center of the inclusion continues to have the highest compressive strain, but now its value is only $\epsilon_{RR} = -0.00054$. It is thus well below the value that was required to vertically align InAs/GaAs SKQDs with at least a 95% probability (−0.00159) and suggests that, when the islands are more realistically simulated by thin slices (instead of spheres) and In segregation is correctly taken into account, even a distance as short as 2 MLs is no longer enough to provide the minimum strain necessary for their effective vertical alignment.

One could of course wonder whether such a small strain value in Fig. 7 — which represents 34% of the value observed in Fig. 2 at 10 nm from the top of the InAs sphere representing a SKQD — would be enough to explain the shorter size and absence of internal periodicity observed in the XSTM images of SMLQDs. It is therefore worth commenting on some relevant differences between SKQDs and SMLQDs. When comparing Figs. 3 and 6, it is clear from Table 1 that, even when the inclusions have the same equivalent volume of InAs material, the strain in the surrounding material is higher for a sphere than for a truncated hemisphere, when calculated at the same distance from the inclusion's surface (2 MLs). This is mainly because, for a sphere, the InAs material is concentrated in a smaller region of space, leading to a higher local strain acting isotropically over longer distances in the surrounding matrix. When the spherical inclusion is covered by GaAs, the maximum tensile strain that can be felt at the top of the flat GaAs surface is located

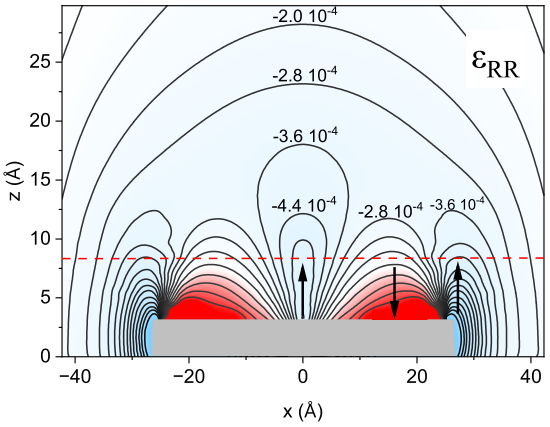

Fig. 7. Distribution of the radial strain ϵ_{RR} in the matrix surrounding a 2D island represented by a thin truncated hemisphere of radius R_0 = 2.5 nm and height h = 0.28 nm. Unlike in Fig. 6, now segregation was taken into account ($R_{seg} = 0.8$), leading to an average compositions of $In_{0.25}Ga_{0.75}As$ and $In_{0.18}Ga_{0.82}As$ for the inclusion and matrix, respectively. The horizontal dashed line represents the matrix's surface, located 2 MLs (0.56*nm*) above the top of the inclusion, where a 2D island of the next InAs submonolayer is supposed to nucleate to form a SMLQD. Red regions indicate tensile strain, i.e., $\epsilon_{RR} > 0$. The increment between adjacent solid isostrain lines is $8x10^{-5}$, and the arrows point toward more positive strain values.

exactly above the center of the sphere, making it more energetically favorable to nucleate the next inclusion. This happens with SKQDs, which can be successfully simulated by spheres, as already shown by Xie et al. [19].

The situation changes considerably when the inclusion has the same volume but is represented by a thin truncated hemisphere — which is more realistic to simulate the 2D islands forming SMLQDs — where the inclusion's material is spread over a longer distance (5 nm in Fig. 6 instead of 2.2 nm in Fig. 3). Fig. 6 shows that the strain distribution is no longer isotropic, and most of it is concentrated close to the periphery of the disk (both in compressive and tensile forms). After covering the inclusion with a few MLs of GaAs, the highest strain at the flat GaAs surface continues to be precisely above the center of the inclusion, forming thus an absolute minimum in the surface potential for the incorporation of the next In atoms. [19] However, this time, there is another local minimum in the surface potential above the periphery of the disk, resulting from the extra tensile strain concentrated there, as shown in Fig. 6. Since the density of 2D islands can be very high (up to 10^{12} cm^{-2}), many of these minima coexist close to each other (the separation between 2D islands can be as small as a few nanometers), and the In atoms of the next InAs layer can be easily driven out of the central minimum [29], leading to irregular In-rich structures embedded in an InGaAs layer, as observed by XSTM.

Finally, In segregation acts in two very different ways during the growth of SKQDs and SMLQDs. InAs SKQDs are large structures containing, nominally, only InAs material and resulting from a self-assembling process when more than 1.7 MLs of InAs are deposited on the GaAs(001) surface. In the course of their formation, some Ga atoms from the substrate are incorporated into the SKQDs to help reduce the total elastic energy of the system [30]. In segregation occurs when such SKQDs are later covered by GaAs, removing In atoms from their outer layers, but keeping a very high In concentration in their core [31,32]. As the manifestations of In segregation are mostly visible in the first 10 MLs of GaAs [27], when the next layer of SKQDs is deposited at a distance z_0 = 10 nm (≈ 36 MLs), the surface is back to pure GaAs and the growth conditions are similar to those of the previous layer of SKQDs. It means that the strain generated by the InAs SKQDs in the surrounding matrix is always at its maximum (nominal) value. On the other hand, SMLQDs are built from the alternated deposition of smaller 2D InAs islands and a few GaAs monolayers. In segregation acts from the very beginning of the cyclic deposition, removing 80% of the In atoms from the 2D islands and scattering them into the next GaAs layers, inside as well as outside the SMLQDs. Since the distance between two consecutive InAs submonolayer is only 2 MLs, the effects of segregation are still very strong when the next deposition of InAs material takes place. As a consequence, the strong In segregation inherent to this kind of heterostructure effectively transforms the nominally highly strained InAs/GaAs system into a weakly strained $In_{0.25}Ga_{0.75}As/In_{0.18}Ga_{0.82}As$ system, as the effective lattice mismatch is reduced by approximately a factor of 14. The resulting strain field, further weakened by the extremely flat geometry of the islands and by the presence of multiple local strain maxima (Fig. 7), is insufficient to impose a unique and energetically favorable nucleation site for subsequent islands. This provides a natural explanation for the absence of robust vertical ordering of the 2D islands observed in high-resolution XSTM measurements, as well as for the formation of the thick $In_{0.10}Ga_{0.90}As$ matrix that accommodates the fraction of In atoms (≈ 20%) diffusing laterally and escaping from the SMLQDs.

The strain calculations presented here are based on isotropic, linear elasticity. While InAs and GaAs are elastically anisotropic cubic crystals, the strong In segregation in SMLQDs leads to smooth compositional gradients and significantly reduces the strain contrast between 2D islands and matrix. As a result, the overall strain amplitudes are small compared to those in nominal InAs/GaAs heterostructures, and the influence of elastic anisotropy and nonlinear effects is correspondingly diminished. Under these conditions, isotropic linear elasticity provides a reliable description of the strain field, and more elaborate models [33] are not expected to alter the central conclusions of this work. While strain plays a central role in driving vertical alignment, the distribution of In during

growth is governed by a complex interplay between strain, surface diffusion, growth rate, and adatom kinetics. In the present work, strain is emphasized because it constitutes the primary energetic driving force for vertical correlation. However, the substantial reduction in strain amplitude caused by strong In segregation, together with this kinetic–thermodynamic interplay, promotes In incorporation at multiple competing sites rather than exclusively above underlying islands, thereby naturally leading to the irregular morphology and limited vertical correlation observed experimentally in XSTM images of SMLQDs.

If one aims to improve the optical and electrical properties of SMLQDs, In segregation must be effectively controlled in order to increase the In content of the 2D islands, thereby enhancing the strain fields and promoting more effective vertical alignment. From a growth perspective, In segregation is a thermally activated process and can therefore be mitigated by lowering the growth temperature. According to Muraki's model [21], reducing the growth temperature from typical values around 500 °C to approximately 375 °C would significantly decrease the segregation coefficient (from 0.80 to 0.57), thereby enhancing the strain field above the islands (from −0.00054 to −0.00171) and promoting effective vertical alignment. Additional strategies, such as increased As overpressure or higher group-III growth rates, may also reduce segregation. However, in all cases, this will happen at the expense of reduced adatom mobility and potentially lower crystal quality, and post-growth annealing may then be required to recover structural quality.

4. Conclusion

Large InAs/GaAs Stranski–Krastanov quantum dots can align vertically in consecutive InAs layers when separated by a GaAs spacer thinner than 10 nm. Since InAs/GaAs submonolayer quantum dots are formed by the alternate deposition of a fraction of an InAs monolayer — leading to the nucleation of a high density of narrow two-dimensional InAs islands — and a few monolayers of GaAs only, one would also expect such islands to form stacks due to the internal strain field. However, high-resolution XSTM data show no evidence of these InAs islands or any internal periodicity, suggesting that In segregation might remove enough In atoms from the nanostructures and considerably weaken the local strain field. In the present work, in an attempt to confirm this assumption, the radial strain ϵ_{RR} was calculated in the matrix around the two-dimensional islands and compared with the minimum strain value necessary to stack Stranski–Krastanov quantum dots ($\epsilon_{RR} = -0.00159$). When the original two-dimensional InAs islands were simulated by small InAs spheres having the same volume and were surrounded by GaAs, the strain estimated 2 MLs above the spherical inclusions was fifteen times higher ($\epsilon_{RR} = -0.0245$). This suggests that they should perfectly stack, contrary to what was observed in XSTM images. When In segregation was added to this simplistic representation of a two-dimensional island, leading to a sphere of $In_{0.25}Ga_{0.75}As$ surrounded by an $In_{0.18}Ga_{0.82}As$ matrix, the strain value was reduced ($\epsilon_{RR} = -0.00220$) but remained larger than that found for SKQDs. However, the situation changed drastically when the two-dimensional islands were more realistically represented by a thin truncated hemisphere — mimicking a disk — in the presence of segregation. In that case, the strain was found to be $\epsilon_{RR} = -0.00054$, which is only 34% of that necessary to fully align InAs/GaAs SKQDs. Such a low strain could be obtained even after covering the two-dimensional islands with only 2MLs of GaAs material, because segregation removes most In atoms from the islands and scatters them into the surrounding matrix, leading to two materials with more similar lattice parameters and, consequently, to much lower local strain. The calculations also revealed that, when this more realistic disk-like shape is adopted, different regions of the surrounding matrix can be under compressive or tensile strain, generating several local minima in the surface potential above the island, which further help spread the In atoms out of the quantum dots. We believe that this work provides important insights into the role of strain and In segregation during the formation of such nanostructures, and clearly shows that segregation must be controlled if one wishes to obtain more robust submonolayer quantum dots.

CRediT authorship contribution statement

T.F. Cantalice: Writing – original draft, Validation, Software, Investigation, Formal analysis. **S.M. Urahata:** Writing – review & editing, Visualization, Validation, Software, Data curation. **A.A. Quivy:** Writing – review & editing, Supervision, Resources, Project administration, Methodology, Funding acquisition, Conceptualization.

Funding

This study was financed in part by the Coordenação de Aperfeiçoamento de Pessoal de Nível Superior - Brasil (CAPES) - Finance Code 001, and by CNPq (grant 309837/2021-9).

Declaration of competing interest

The authors declare that they have no known competing financial interests or personal relationships that could have appeared to influence the work reported in this paper.

Data availability

Data will be made available on request.

References

[1] I.L. Krestnikov, N.N. Ledentsov, A. Hoffmann, D. Bimberg, Arrays of two-dimensional islands formed by submonolayer insertions: Growth, properties, devices, Phys. Stat. Sol. (A) 183 (2001) 207–233, http://dx.doi.org/10.1002/1521-396X(200102)183:2<207::AID-PSSA207>3.0.CO;2-2.

[2] D. Leonard, M. Krishnamurthy, C.M. Reaves, S.P. Denbaars, P.M. Petroff, Direct formation of quantum-sized dots from uniform coherent islands of InGaAs on GaAs surfaces, Appl. Phys. Lett. 63 (1993) 3203–3205, http://dx.doi.org/10.1063/1.110199.

[3] A. Lenz, H. Eisele, J. Becker, J.-H. Schulze, T.D. Germann, F. Luckert, K. Pötschke, E. Lenz, L. Ivanova, A. Strittmatter, D. Bimberg, U.W. Pohl, M. Dähne, Arrays of two-dimensional islands formed by submonolayer insertions: Growth, properties, devices, J. Vac. Sci. Technol. B 29 (2011) 04D104, http://dx.doi.org/10.1116/1.3602470.

[4] G.R. Bell, T.J. Krzyzewski, P.B. Joyce, T.S. Jones, Island size scaling for submonolayer growth of InAs on GaAs(001)-(2x4): strain and surface reconstruction effects, Phys. Rev. B 61 (2000) R10551, http://dx.doi.org/10.1103/PhysRevB.61.R10551.

[5] A. Alzeidan, M.S. Claro, A.A. Quivy, High-detectivity infrared photodetector based on InAs submonolayer quantum dots grown on GaAs(001) with a 2× 4 surface reconstruction, J. Appl. Phys. 126 (2019) 224506, http://dx.doi.org/10.1063/1.5125238.

[6] R.C. Roca, I. Kamiya, Photoluminescence tuning of stacked submonolayer (sml) inas nanostructures across the 2d to 3d transition, Appl. Phys. Lett. 118 (2021) 183104, http://dx.doi.org/10.1063/5.0047287.

[7] J. Zhang, K. Han, S. Ma, Z. Zhuo, R. Cheng, Y. Zhou, Y. Wang, P. Gao, B. Xu, Tuning the optical properties of 3-period inas/gaas sml-qds by varying inas deposition amount, Micro Nanostructures 210 (2025) 208488, http://dx.doi.org/10.1016/j.micrna.2025.208488.

[8] H. Ghadi, S. Sengupta, S. Shetty, A. Manohar, A. Balgarkashi, S. Chakrabarti, N.B. Pendyala, S.L. Prajapati, A. Kumar, Comparison of three design architectures for quantum dot infrared photodetectors: InGaAs-capped dots, dots-in-a-well, and submonolayer quantum dots, IEEE Trans. Nanotechnol. 14 (2015) 603, http://dx.doi.org/10.1109/TNANO.2015.2432044.

[9] T. Borrely, A. Alzeidan, M.D. de Lima, G.M. Jacobsen, T.-Y. Huang, Y.-C. Yang, T.F. Cantalice, R.S. Goldman, M.D. Teodoro, A.A. Quivy, Viability of intermediate band solar cells based on InAs/GaAs submonolayer quantum dots and the role of surface reconstruction, Sol. Energy Mater. Sol. Cells 254 (2023) 112281, http://dx.doi.org/10.1016/j.solmat.2023.112281.

[10] W.S. Liu, T.K. Yang, M.E. Hsu, K.Y. Hsu, B. Kondapavuluri, J.I. Chyi, Fabrication of inas 2d submonolayer nanostructure-based solar cells with ingaas/gaassb double-well structure, Opt. Mater. 159 (2025) 116576, http://dx.doi.org/10.1016/j.optmat.2024.116576.

[11] S. Choudhary, S. Dongre, D. Panda, D. Das, S. Chakrabarti, Investigation of inter-dot tunnelling effect in hybrid coupled qds heterostructures for short-wave infrared detection (swir) application, J. Alloy. Compd. 1010 (2025) 177612, DOI.

[12] S.J. Addamane, A. Laurain, C.W. Baker, T.J. Rotter, J. Watt, J.L. Reno, G. Balakrishnan, J.V. Moloney, Submonolayer quantum-dot based saturable absorber for femtosecond pulse generation, J. Electron. Mater. 50 (2021) 2710, http://dx.doi.org/10.1007/s11664-021-08795-x.

[13] D. Guo, J. Huang, M. Benamara, Y.I. Mazur, Z. Deng, G.J. Salamo, High operating temperature mid-infrared ingaas/gaas submonolayer quantum dot quantum cascade detectors on silicon, IEEE J. Quantum Electron. 59 (2023) 2300106, http://dx.doi.org/10.1109/JQE.2023.3238754.

[14] N. Alnami, R. Kumar, A.V. Kuchuk, Y. Maidaniuk, S.K. Saha, A.A. Alnami, R. Alhelais, A. Kawagy, M.E. Ware, Y.I. Mazur, G.J. Salamo, Inas nanostructures for solar cell: Improved efficiency by submonolayer quantum dot, IEEE J. Quantum Electron. 59 (2023) 2300106, http://dx.doi.org/10.1109/JQE.2023.3238754.

[15] Z. Shen, Z. Deng, X. Zhao, J. Huang, C. Cao, X. Zou, F. Liu, Q. Gong, B. Chen, Submonolayer quantum dot quantum cascade long-wave infrared photodetector grown on ge substrate, Appl. Phys. Lett. 118 (2021) 081102, http://dx.doi.org/10.1063/5.0038844.

[16] R.S.R. Gajjela, A.L. Hendriks, A. Alzeidan, T.F. Cantalice, A.A. Quivy, P.M. Koenraad, Cross-sectional scanning tunneling microscopy of InAs/GaAs(001) submonolayer quantum dots, Phys. Rev. Mater. 4 (2020) 114601, http://dx.doi.org/10.1103/PhysRevMaterials.4.114601.

[17] T.F. Cantalice, A. Alzeidan, S.M. Urahata, A.A. Quivy, In-situ measurement of indium segregation in InAs/GaAs submonolayer quantum dots, Mater. Res. Express 6 (2019) 126205, http://dx.doi.org/10.1088/2053-1591/ab55a8.

[18] T.F. Cantalice, A. Alzeidan, G.M. Jacobsen, T. Borrely, M.D. Teodoro, A.A. Quivy, Evidence of weak strain field in InAs/GaAs submonolayer quantum dots, micro and nanostructures, Micro Nanostructures 172 (2022) 207449, http://dx.doi.org/10.1016/j.micrna.2022.207449.

[19] Q. Xie, A. Madhukar, P. Chen, N.P. Kobayashi, Vertically self-organized inas quantum box islands on gaas(100), Phys. Rev. Lett. 75 (1995) 2542, http://dx.doi.org/10.1103/PhysRevLett.75.2542.

[20] G. Raino, A. Salhi, V. Tasco, M.D. Vittorio, A. Passaseo, R. Cingolani, M.D. Giorgi, E. Luna, A. Trampert, Structural and optical properties of vertically stacked triple inas dot-in-well structure, J. Appl. Phys. 103 (2008) 096107, http://dx.doi.org/10.1063/1.2921266.

[21] K. Muraki, S. Fukatsu, Y. Shiraki, R. Ito, Surface segregation of In atoms during molecular beam epitaxy and its influence on the energy levels in InGaAs/GaAs quantum wells, Appl. Phys. Lett. 61 (1992) 557–559, http://dx.doi.org/10.1063/1.107835.

[22] S. Martini, A.A. Quivy, E.C.F. da Silva, J.R. Leite, Real-time determination of the segregation strength of indium atoms in InGaAs layers grown by molecular-beam epitaxy, Appl. Phys. Lett. 81 (2002) 2863, http://dx.doi.org/10.1063/1.1513182.

[23] S. Martini, A.A. Quivy, T.E. Lamas, M.J. da Silva, E.C.F. da Silva, J.R. Leite, Influence of indium segregation on the RHEED oscillations during the growth of InGaAs layers on a GaAs(001) surface, J. Cryst. Growth 251 (2003) 101–105, http://dx.doi.org/10.1016/S0022-0248(02)02313-8.

[24] A.L. Kolesnikova, M.Y. Gutkin, A.E. Romanov, Analytical elastic models of finite cylindrical and truncated spherical inclusions, Int. J. Solids Struct. 143 (2018) 59–72, http://dx.doi.org/10.1016/j.ijsolstr.2018.02.032.

[25] N.F. Mott, F.R.N. Nabarro, An attempt to estimate the degree of precipitation hardening, with a simple model, Proc. Phys. Soc. 52 (1940) 86, http://dx.doi.org/10.1088/0959-5309/52/1/312.

[26] J. Salençon, Handbook of Continuum Mechanics - General Concepts, Thermoelasticity, Springer Berlin, Heidelberg, 2001, http://dx.doi.org/10.1007/978-3-642-56542-7.

[27] S. Martini, A.A. Quivy, M.J. da Silva, T.E. Lamas, E.C.F. da Silva, J.R. Leite, E. Abramof, Ex-situ investigation of indium segregation in InGaAs/GaAs quantum wells using high-resolution x-ray diffraction, J. Appl. Phys. 94 (2003) 7050, http://dx.doi.org/10.1063/1.1621738.

[28] A. Alzeidan, T.F. Cantalice, K.E. Sautter, K.D. Vallejo, P.J. Simmonds, A.A. Quivy, High-performance infrared photodetector based on inas/gaas submonolayer quantum dots grown at high temperature with a (2× 4) surface reconstruction, Sensors Actuators A: Phys. 374 (2024) 115464, http://dx.doi.org/10.1016/j.sna.2024.115464.

[29] J. Tersoff, C. Teichert, M.G. Lagally, Self-organization in growth of quantum dot superlattices, Phys. Rev. Lett. 76 (1996) 1675, http://dx.doi.org/10.1103/PhysRevLett.76.1675.

[30] P.B. Joyce, T.J. Krzyzewski, G.R. Bell, B.A. Joyce, T.S. Jones, Composition of InAs quantum dots on GaAs(001): Direct evidence for In/GaAs alloying, Phys. Rev. B 58 (1998) R15981, http://dx.doi.org/10.1103/PhysRevB.58.R15981.

[31] J.G. Keizer, A.B. Henriques, A.D.B. Maia, A.A. Quivy, P.M. Koenraad, Atomically resolved study of the morphology change of InAs/GaAs quantum dot layers induced by rapid thermal annealing, Appl. Phys. Lett. 101 (2012) 243113, http://dx.doi.org/10.1063/1.4770371.

[32] R.Y. Tanaka, N.M. Abe, E.C.F. da Silva, A.A. Quivy, Modeling the 3D in profile of $In_xGa_{1-x}As$/GaAs quantum dots, J. Phys. D - Appl. Phys. 49 (2016) 215101, http://dx.doi.org/10.1088/0022-3727/49/21/215101.

[33] V.A. Shchukin, D. Bimberg, V.G. Malyshkin, N.N. Ledentsov, Vertical correlations and anticorrelations in multisheet arrays of two-dimensional islands, Phys. Rev. B 57 (1998) 12262, http://dx.doi.org/10.1103/PhysRevB.57.12262.